Crystallization-Induced Interconnected Structure in Semicrystallizable Polyester/Polyether Binary Blends

Natalia V. Pogodina, Young Gyu Jeong, Suriyakala Ramalingam, Cuihong Jiang, and Shaw Ling Hsu*

Polymer Science and Engineering Department, and Materials Research Science and Engineering Center, University of Massachusetts, Amherst, Massachusetts 01003

Charles W. Paul

National Starch and Chemical, Bridgewater, New Jersey 08807

Received April 18, 2006; Revised Manuscript Received July 13, 2006

ABSTRACT: The viscosity of binary blends containing one crystallizable component has been analyzed. The elastic moduli of these phase-separated blends exhibit extremely interesting discontinuities as a function of the overall sample composition. These abrupt changes cannot be attributed to the volume fraction of the crystallizable polyester-rich domains but rather to the extremely small amount (∼2% polyester) of unusual needle-shaped crystallites in the polyester-poor regions and interactions between domains and matrix. Therefore, the overall mechanical property of the binary blend must be considered in terms of the volume fraction of the polyester-rich domains interconnected by these unusual polyester-poor regions.

Introduction

Single-component polyurethanes used for coatings or adhesives are extremely interesting from both fundamental and practical perspectives. For these applications, functionalized polyethers and polyesters are formed and blended with a third component to address processing issues.[1−4] The one-component ternary polymer blend incorporating isocyanates can then react with moisture in the environment to form the final product. The blends typically consist of a polyether because of elastic properties and a crystallizable polyester as the formed crystallites can be used to control the viscosity of the formulation during application. An acrylic copolymer is usually added to the blend system to control miscibility behavior and enhance performance at elevated temperatures.

These types of reactive blends have been studied extensively in our laboratory. Our previous studies focused on formation of prepolymers,[5] the phase behavior of binary or ternary blends,[6−9] the phase separation kinetics,[10,11] the morphological features formed during phase separation, and the crystallization process that may occur concurrently.[12−14] The viscosity change as a function of temperature, time, and composition has attracted our interest recently. The multistep change in viscosity is directly correlated to the local chain dynamics of the acrylate and the crystallization process associated with the polyester.[7,12,15] These are expected, yet the details of change for a number of miscible or immiscible systems remain to be analyzed.

This study focused on the unusual viscosity changes observed in rheological measurements. As described above, the ternary blend systems are the norm. Even at elevated temperatures, however, the blends may not achieve fully miscible mixtures. Depending on the polyester chemical structure, these components can phase-separate into polyester-rich spherical domains and the polyester-poor matrix. As expected, when the temperature of the blend is lowered from melt, the polyesters crystallize in two types of regions (domains and the matrix) at different rates and to different degrees of crystallinity. By following the temperature profile, it is possible to use time-resolved infrared measurements to follow the concurrent crystallization process in the polymer blends, thus establishing a qualitative understanding of the viscosity change.[13,15]

It is not possible, however, to analyze the viscosity increase in a quantitative fashion using existing theories applicable to particulate-filled polymeric composites. One of the earliest theories for a composite system was developed for elastomers and based on Einstein's equation for the viscosity of a suspension of rigid spherical inclusions.[16] In this equation, the stiffening mechanism is dependent only on the volume fraction of particles and independent of particle size. In our system, abrupt changes in viscosity as a function of composition require additional consideration. The crystallization kinetics and degree of crystallinity achieved as well as the shape of the crystallites formed in the poor phase can be controlling factors in the overall rheological response. Furthermore, the polyester-poor matrix region provides the connectivity of spherical domains, a factor that must be considered. Similar behavior has been seen in the sorbitol/polyolefin system.[17−21] In that case, electron microscopy has revealed the presence of long fibers that increase the viscosity of polyolefin melt.[17,19,21]

Additional analyses of the viscosity change have been carried out. Since the role of the acrylate is better understood, we concentrate on binary blends of nonfunctional components involving noncrystallizable polyether, poly(propylene glycol) (PPG), and crystallizable aliphatic polyester, poly(hexamethylene adipate) (PHMA). Unlike other polyesters studied, this polyether/polyester pair is immiscible and exhibits liquid−liquid phase separation at all compositions even in the molten state. When cooled from the molten phase, the size of phase-separated structures does not change.[13] Only the degree of crystallinity within the two regions increases as a function of time. It is the structure within the polyester-poor region that exhibits much influence on overall sample viscosity. Our analyses are reported here.

* To whom correspondence should be addressed: tel 413-577-1125; e-mail slhsu@polysci.umass.edu; fax 413-545-0082.

10.1021/ma060868v CCC: $33.50 © 2006 American Chemical Society
Published on Web 08/24/2006

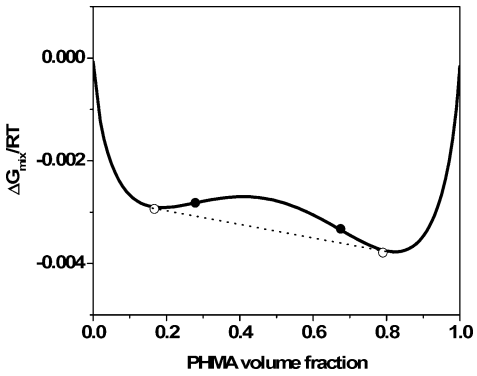

Figure 1. Free energy of mixing as a function of composition for PHMA/PPG binary blends at 120 °C. The binary interaction parameter $\chi = 0.0647$ at 120 °C.[6] The filled and open circles indicate spinodal and bimodal points, respectively. The dotted line represents the coexistence curve.

Table 1. Characteristics of Raw Components in Binary Blends

blend component	M_w (g/mol)	M_w/M_n	T_m (°C)	T_g (°C)
PHMA	2505	1.59	54.5	−61.0
PPG	1906	1.01		−66.0

Experimental Section

As in our previous studies, polyether [poly(propylene glycol) (PPG)] and crystallizable aliphatic polyester [poly(hexamethylene adipate) (PHMA)] were used as two components for binary blends. Their physical properties are listed in Table 1. Binary blends with various compositions were prepared by melt-mixing at 120 °C, and the compositions were varied by changing the volume fraction of PHMA (φ) from 0.02 to 0.5.

An optical microscope (Olympus Vanox) equipped with a digital camera and custom-designed temperature controller was used for the morphological studies in the melt and during crystallization. All crystallization experiments were followed using the birefringence developed for samples between two polarizers with an orthogonal polarization axis.

The composition and degree of crystallinity of the PHMA-rich and PHMA-poor phase as well as the average composition and average degree of crystallinity of the blends were determined using previously developed spectroscopic and calorimetric methods.[12,13,15]

Rheological experiments were performed on an Advanced Rheometric Expansion System (ARES) of Rheometric Scientific Inc. (RSI), equipped with cone and plate and parallel plates (diameter 25 mm). The instrument is operated using RSI Orchestrator software, version 6.3.0. Studies were conducted in the small-amplitude oscillatory shear (SAOS) mode. Frequency sweeps were performed in a window of 0.1−10 rad/s (5 points/decade) at a single temperature $T = 40$ °C and strain amplitude of 1%. The experimental temperature $T = 40$ °C was specifically chosen below the PHMA melting temperature $T_m = 58$ °C in order to examine effects of the PHMA crystallites during frequency sweeps. Crystallization kinetic studies with temperature/time sweeps from 120 to 40 °C have also been investigated at a constant frequency of 5 rad/s. Here the initial strain amplitude of 20% was manually decreased as temperature decreased to stay below the maximum measurable torque of our instrument.

Results and Discussion

Based on experimental studies, the free energy of mixing as a function of composition is shown in Figure 1. Blends with the volume fraction of PHMA φ in the range from 0.02 to 0.5 were studied. All PHMA/PPG blends, prepared by melt-mixing and in the probed composition range, showed distinct phase-separated morphology with spherical PHMA-rich domains dispersed in the PPG-rich matrix (bicontinuous morphology for $\varphi = 0.5$ blends).[12] Our detailed spectroscopic studies showed

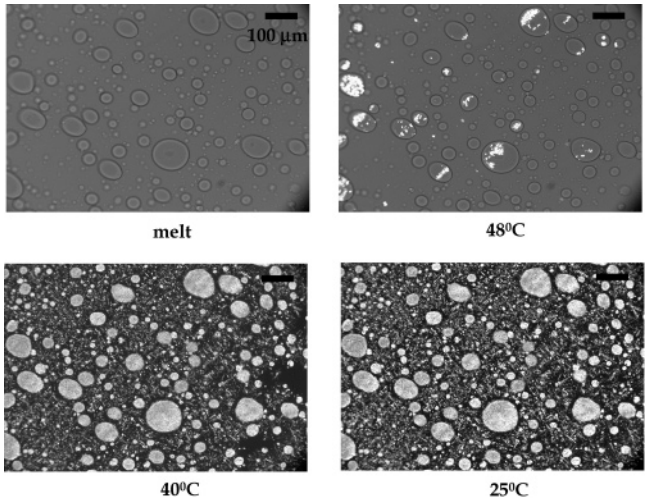

Figure 2. Optical micrographs for the $\varphi = 0.2$ PHMA/PPG blend cooled from the melt to room temperature 25 °C. The scale bar is 100 μm.

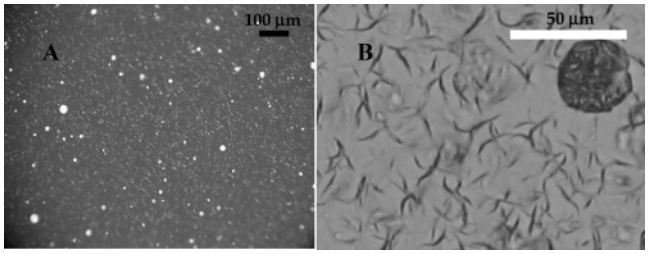

Figure 3. Optical micrographs for the $\varphi = 0.02$ PHMA/PPG blend taken at room temperature 25 °C. The scale bar is 100 μm in (A) and 50 μm in (B).

that PHMA concentration in each phase is a function of blend composition.[12] With decreasing the overall PHMA content in blends, PHMA concentration in a PHMA-rich phase increases and reaches 74% for the PHMA/PPG-10/90 blend, while decreasing in a PHMA-poor phase and reaching about 5% for the same PHMA/PPG-10/90 blend.

Optical micrographs were taken in the melt and upon cooling to room temperature from the PHMA/PPG −20/80 blend ($\varphi = 0.2$) in the melt, shown in Figure 2. Polyester-rich spherical domains have a very broad size distribution with the diameter ranging from ∼0.1 to 10 μm or even larger. PHMA crystallites in domains are seen as whitish regions that emerge near the interface and, with time, grow radially inward. The crystallization of PHMA in the PPG-rich matrix occurs at a later time and at a much slower rate in comparison to that in the PHMA-rich domains. PHMA crystals in the PPG-rich matrix are seen as fine needles or leaf-like (Figure 2). Thus, the crystallization of PHMA/PPG blends consists of two processes: the fast crystallization in the PHMA-rich phase (spherical domains) and slow formation of elongated leaf-shaped crystals in a PPG-rich matrix.

Figure 3 shows optical micrographs of the PHMA/PPG blend with $\varphi = 0.02$ at room temperature. It is noted that the PHMA-rich spherical domains are reduced in size and number compared with that of the PHMA/PPG blend with $\varphi = 0.2$, indicating that the size and number of such domains are strongly dependent on blend composition. More importantly, for the $\varphi = 0.02$ PHMA/PPG blend, the dominating shape of PHMA crystallites in the matrix is fine needle- or leaf-like, as seen in the magnified image Figure 3B. Additional analysis of crystallization kinetics is correlated to rheological data as shown below.

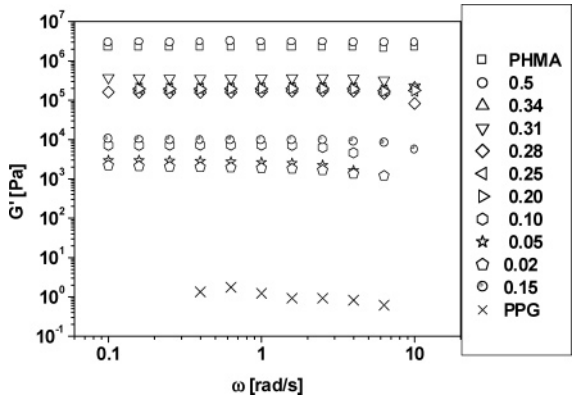

Figure 4. Storage (elastic) modulus G' as a function of frequency ω for PHMA/PPG blends at different composition.

In small-amplitude oscillatory shear (SAOS) the dynamic moduli are expressed as in-phase (G') and out-of phase (G'') components of the sinusoidal stress τ

$$\tau = \tau_0 \sin(\omega t + \delta) = G'\gamma_0 \sin \omega t + G''\gamma_0 \cos \omega t \quad (1)$$

$$\tan \delta = \frac{G''}{G'} \quad (2)$$

Here γ_0 is the amplitude of the imposed strain and δ is the phase (loss) angle between strain and stress. G' and G'' are the storage and viscous modulus, respectively. The ratio between dissipated and stored energy is expressed by the loss tangent δ. We concentrate on the behavior of the elastic (storage) modulus. At the critical gel point, the low-frequency dynamic moduli show power-law behavior[22,23]

$$G'_c = \frac{G''_c}{\tan \delta_c} = S_c \Gamma(1 - n_c) \cos\left(\frac{n_c \pi}{2}\right) \omega^{n_c} \quad (3)$$

Here S_c and n_c are the gel stiffness and the relaxation exponent and Γ is the gamma function. A consequence of this power-law behavior (at the gel point) is a frequency-independent loss tangent in the terminal zone. This frequency independence provides a most reliable and generally valid method for determining the permanent network, critical gel, or gel-like structure.

$$\tan \delta_c = \tan\left(\frac{n_c \pi}{2}\right) = \text{const} \quad (4)$$

A frequency sweep experiment was performed for PHMA/PPG blends in a frequency window from 0.1 to 10 rad/s at 40 °C. Figures 4 and 5 show the evolution of the elastic (storage) modulus G' and tan δ as a function of frequency for PHMA/PPG blends at increasing volume fraction of PHMA. It is important to emphasize several points. First, there is no frequency dependence of the storage modulus in the probed frequency range. Generally speaking, for the monodisperse polymer melts as well as the low concentrated suspensions, the storage modulus scales with frequency in the terminal zone in a power of 2 and loss modulus in a power of 1, that is, $G' \sim \omega^2$ and $G'' \sim \omega$.[24] Thus, the absence of frequency dependence indicates strong interactions and connectivity in the suspension-like system. The region where G' remains constant is usually referred to as a "rubber plateau". In this case such a plateau covers the entire probed frequency range of 2 decades, a strong indication of interchain connectivity, i.e., physical cross-linking. Second, there are two dramatic increases in the elastic modulus

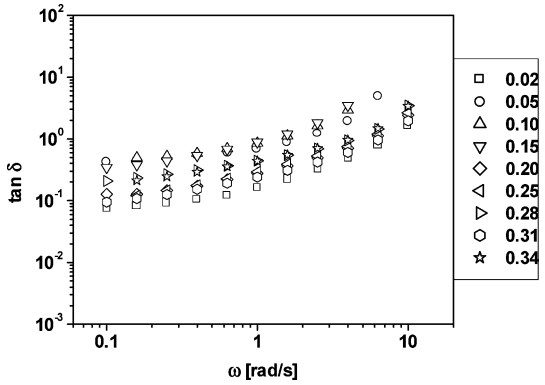

Figure 5. Loss tangent as a function of frequency ω for PHMA/PPG blends at different composition.

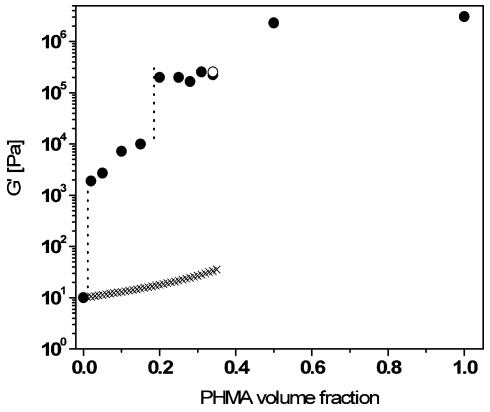

Figure 6. Storage modulus G' as a function of PHMA volume fraction in PHMA/PPG blends (semilogarithmic plot). Open circle indicates the ternary blend PHMA/PPG/Acr-34/33/33 (Acr = acrylic copolymer). The cross line is from the composite model calculation.

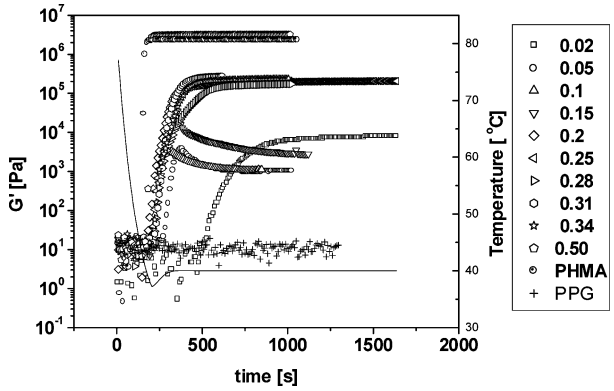

Figure 7. Time and temperature dependence of the storage modulus G' for PHMA/PPG blends with various PHMA content. The solid line represents the temperature profile upon cooling from the melt to 40 °C.

G' with increase of PHMA content for blends with 2% and 20% PHMA (Figure 6), in comparison with G' of pure PPG. Figure 7 plots the elastic modulus G' of blends at a frequency $\omega = 1$ rad/s as a function of blend composition (i.e., PHMA volume fraction). Two discontinuities were clearly observed for G' with 2% and 20% volume fractions of PHMA. It also should be noted that in the low-frequency range the values of loss tangent (Figure 5) are below one for all blends studied. This may indicate dominating solidlike behavior of PHMA/PPG blends.

It is possible to analyze these rheological data by considering that a PHMA/PPG system behaves similarly to a suspension of hard spheres (crystallized spherical PHMA domains) in an amorphous PPG matrix. This is based on the following

CDV

considerations: (1) during crystallization, the spherical domains do not grow in size, (2) crystallization starts from the interface of domains/matrix, and (3) crystallization occurs in the confined geometry. For a suspension of rigid spherical inclusions (PHMA crystallized fillers) in a PPG matrix, the shear modulus G' can be expressed by the modified Kerner equation[25]

$$\frac{G'_{\text{blend}}}{G'_1} = \frac{1 + AB\varphi}{1 - B\psi\varphi} \tag{5}$$

where

$$A = \frac{7 - 5\nu_1}{8 - 10\nu_1} \quad \text{and} \quad B = \frac{G'_2/G'_1 - 1}{G'_2/G'_1 + A} \tag{6}$$

Here G'_1 and G'_2 are the shear moduli of the matrix and filler, respectively, φ is the volume fraction of PHMA filler, and ν_1 is the Poisson's ratio of the matrix. The factor ψ depends on the maximum packing fraction of the filler $\varphi_{\max}$ (for the simple cubic lattice packing $\varphi_{\max} = 0.52$) and is given by

$$\psi = 1 + \frac{(1 - \varphi_{\max})\varphi}{\varphi_{\max}^2} \tag{7}$$

The factor A is related to the generalized Einstein coefficient K_E by

$$A = K_E - 1 \tag{8}$$

where $K_E = 2.5$ for rigid spheres in a matrix with Poisson's ratio $\nu_1 = 0.5$. Using $K_E = 2.5$, $\nu_1 = 0.5$, and eqs 7 and 8, we have $A = 1.5$ and $\psi = 1.35$ for the blend with PHMA volume fraction $\varphi = 0.2$.

The shear modulus of the crystallized pure PHMA is $G'_2 = 5 \times 10^6$ Pa while for the amorphous pure PPG matrix it is 5 orders of magnitude lower, which gives $B = 1$ and from eq 5 the ratio $G'_{\text{blend}}/G'_1 = 1.8$. Thus, according to a composite model, for a PPG matrix filled up to 20% with spherical rigid (crystallized) PHMA inclusions, we can expect an increase in G'_{blend} of about 80% relative to the unfilled PPG matrix. The theoretical values of G'_{blend} from the composite model are shown in Figure 6 as a crossed line. Clearly, Figure 6 shows that our experimental results are not in agreement with this expectation. Experimental G' values of PHMA/PPG blends with all studied compositions including PHMA content as low as 2% exceed the G'_1 values of the unfilled PPG matrix by 3−4 orders of magnitude. Such high elasticity cannot be explained in terms of a composite model of isolated fillers. This result suggests that the high G' values of PHMA/PPG blends originate from strong interactions between PHMA domains and the PPG matrix which promote connectivity, i.e., network formation.

The network that we hypothesize can be formed in different ways, and its morphology strongly depends on blend miscibility and blend composition, i.e., volume fraction of the dispersed PHMA phase and strength of interchain interactions. Other influencing factors include thermal history, cooling rate, crystallization temperature, applied shear stress, phase separation kinetics, dispersion of formed domains, and others. With a sufficiently high volume fraction of PHMA in the blend (as our results showed about 20% PHMA) an interconnected network of spherical domains is formed. This transition can be understood as "percolation". The critical volume fraction of the inclusions when the spanning network first appears is then the percolation threshold. At the percolation threshold, system properties dramatically change: the cluster size diverges to infinity, and the elasticity shoots up.

The percolation theory predicts that a random distribution of monodisperse spheres displays the onset of percolation in the range of volume fractions 0.28−0.156 depending on whether overlapping or nonoverlapping spheres are considered.[26] Thus, the range of the percolation threshold is broad even for monodisperse spheres. The condition of monodispersity is not applicable to PHMA/PPG blends discussed here. As mentioned above, the blends possess a significant domain size distribution. Thus, taking into account the polydispersity of the size distribution and complexity of the system, our experimental result $\varphi = 0.2$ is in good agreement with the percolation threshold for spheres.[26]

The percolation threshold is a strong function of the "domain" aspect ratio and can be decreased by an order of magnitude for randomly oriented ellipsoids/needles with a high aspect ratio as compared to spherical domains.[26] Figure 6 clearly shows a step increase in value of the elastic modulus G' for blends with only 2% PHMA. Thus, we conclude that in this case an interconnected network is also formed. However, unlike the above-mentioned spherical-domain network, the morphology of this network consists of fine needle- or leaf-like crystals, as discussed earlier (see Figure 3). These needles may percolate even at low volume fractions of 0.02 if they possess a sufficiently high aspect ratio which enhances interchain interactions and promotes connectivity. Indeed, this is the case. The small size of the crystallites and softness of the surrounding amorphous phase give rise to the high mobility of these cross-links, resulting in high solid-state elasticity. Thus, two networks are formed in PHMA/PPG blends: at very low PHMA content the needle-like low crystalline (crystallinity ∼3%) network is formed, while around 20% PHMA the high crystalline (crystallinity ∼40%) network of percolating spherical domains is additionally formed. Both networks are reversible; i.e., cross-links can be destroyed at elevated temperatures.

The blend starts as a liquid then transforms into a viscoelastic solid as a function of time. Previous studies indicated there is a direct correlation between viscosity changes and the polyester crystallization process in polymer blends.[12,15] The increase of $G'(T,t)$ during crystallization of PHMA homopolymer and various PHMA/PPG blends as a function of time is shown in Figure 7. Such crystallization behavior allows a separation of the onset of crystallization from the crystal growth kinetics. The increase of the storage modulus follows a sigmoidal curve. The time for nuclei to form is defined as the induction time during which the storage modulus has a constant value. The slope of the $G'(t)$ sigmoidal curve at the inflection point is related to the "crystallization rate". In our analysis, nucleation and crystallization rates were normalized by the maximum nucleation/crystallization rate, monitored for pure PHMA.

Figure 8 shows the dependence of normalized nucleation and crystallization rates on the volume fraction of PHMA in blends. As the PHMA content decreases, the crystallization temperature $T_{c(\text{PHMA})}$ decreases and the crystallization profile of the PHMA/PPG blends becomes slower and broader, which is reflected in the slower crystallization rates. It should be noted that the crystallization rates change in a much broader range spanning several decades as compared to the nucleation rates. It is not surprising that the nucleation rate is a relative constant value as the local concentration, the governing factor for nucleation, does not change significantly with blend composition. On the other hand, the "crystal growth" exhibits a change in rate at $\varphi = 0.15$ or greater. It should be noted these values are obtained

CDV

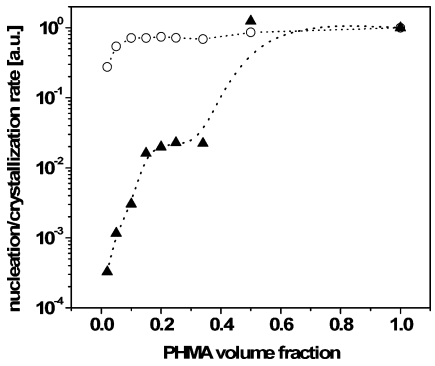

Figure 8. Crystallization rates (solid triangles) and nucleation rates (open circles) for PHMA/PPG blends as a function of PHMA volume fraction φ. Crystallization/nucleation rates are normalized with the maximum crystallization/nucleation rate of the pure PHMA.

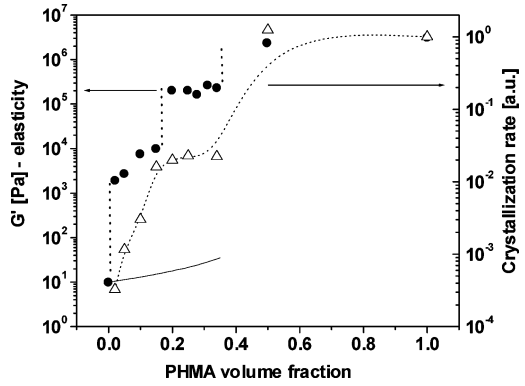

Figure 9. Storage modulus G' (solid circles) and crystallization rates (open triangles) of PHMA/PPG binary blends as a function of PHMA volume fraction φ. The solid line represents the calculated results based on the composite model.

from storage modulus values. Therefore, at $\varphi = 0.15$ or greater, a network and thus a constant modulus value is achieved. This physical network is maintained until the bicontinuous network is formed at high PHMA content.

When percolation occurs, the crystallization kinetics and sample elasticity are governed not by the individual contributions of the dispersed domains but by the response from the network. This response from the whole network is constant inside the percolation region $\varphi = 0.2-0.4$ and is expressed in the constant elasticity (G' values) and constant crystallization rates (Figure 9). Thus, we introduce several methods to detect the percolation limit: step increase in elasticity at a specific volume fraction of the dispersed phase, high constant elasticity values, and constant crystallization rates in the composition range that marks the percolation regime. At higher volume fractions $\varphi > 0.4$, the morphology becomes bicontinuous and the dispersed morphology is lost as is the percolation.

Conclusions

Rheological data obtained in small-amplitude oscillatory modes for PHMA/PPG immiscible blends were directly correlated to the crystallization behavior within each phase-separated structure, PHMA-rich domains and the PHMA-poor matrix. The volume fraction of PHMA was varied from $\varphi = 0.02$ to 0.5. Upon cooling the blends below the melting temperature of PHMA, a high elastic behavior was observed. The composite model of isolated fillers randomly dispersed in a matrix does not adequately describe the rheological behavior and high elasticity in our system. A step increase of elasticity at $\varphi = 0.2$ PHMA is explained in terms of the percolation of crystallized spherical domains (reduction of the free phase volume). The unusual high elasticity at very low PHMA volume fraction $\varphi = 0.02$ is attributed to the network of needle-shape PHMA crystallites in the PPG-rich matrix.

Thus, our data can only be explained by the presence of two networks formed in PHMA/PPG blends. At very low PHMA content the needle-shaped low crystalline (crystallinity ~3%) network is formed. At ~20% PHMA the high crystalline (crystallinity ~40%) network of percolating spherical domains is formed in addition to the first one. Both networks are physical in nature and can be destroyed upon heating, unlike chemical cross-linking. The range of blend compositions, where high elasticity and crystallization rates are independent of PHMA volume fraction, marks the percolation region. It should be emphasized that the origin of the low crystalline percolating network, formed at very low PHMA content, is not clear and need be further explored. The nature of interchain interactions leading to interconnectivity at such low PHMA content also needs to be addressed.

References and Notes

(1) de Genova, R.; Grier, L.; Murray, P.; Clay, W. *Tappi J.* **1998**, *6*, 196.
(2) Szycher, M. *Szycher's Handbook of Polyurethanes*; CRC Press: Boca Raton, FL, 1999.
(3) Forschner, T. C.; Gwyn, D. E.; Xiao, H. X.; Suthar, B.; Sun, L. Q.; Frisch, K. C. *Adhes. Age* **1999**, *42*, 20.
(4) Vick, C. B.; Okkonen, E. A. *For. Prod. J.* **1998**, *48*, 71.
(5) Heintz, A. M.; Duffy, D. J.; Hsu, S. L.; Suen, W.; Chu, W.; Paul, C. W. *Macromolecules* **2003**, *36*, 2695.
(6) Duffy, D. J.; Stidham, H. D.; Hsu, S. L.; Sasaki, S.; Takahara, A.; Kajiyama, T. *J. Mater. Sci.* **2002**, *37*, 4851.
(7) Jeong, Y. G.; Ramalingam, S.; Archer, J.; Hsu, S. L.; Paul, C. W. *J. Phys. Chem. B* **2006**, *110*, 2541.
(8) Duffy, D. J.; Heintz, A. M.; Stidham, H. D.; Hsu, S. L.; Suen, W.; Chu, W.; Paul, C. W. *J. Adhes.* **2003**, *79*, 1091.
(9) Duffy, D. J.; Heintz, A. M.; Stidham, H. D.; Hsu, S. L.; Suen, W.; Paul, C. W. *Int. J. Adhes. Adhes.* **2005**, *25*, 39.
(10) Meuse, C. W.; Tao, H.-J.; Hsu, S. L.; MacKnight, W. J. *Polym. Prepr. (Am. Chem. Soc., Div. Polym. Chem.)* **1993**, *34*, 266.
(11) Lee, H. S.; Hsu, S. L. *Macromolecules* **1989**, *22*, 1100.
(12) Jeong, Y. G.; Pagodina, N. V.; Jiang, C.; Hsu, S. L.; Paul, C. W. *Macromolecules* **2006**, *39*, 4907.
(13) Hashida, T.; Jeong, Y. G.; Hua, Y.; Hsu, S. L.; Paul, C. W. *Macromolecules* **2005**, *38*, 2876.
(14) Jeong, Y. G.; Hashida, T.; Hsu, S. L.; Paul, C. W. *Macromolecules* **2005**, *38*, 2889.
(15) Jeong, Y. G.; Hashida, T.; Wu, G.; Hsu, S. L.; Paul, C. W. *Macromolecules* **2006**, *39*, 274.
(16) Ahmed, S.; Jones, F. R. *J. Mater. Sci.* **1990**, *25*, 4933.
(17) Kristiansen, M.; Werner, M.; Tervoort, T.; Smith, P.; Blomenhofer, M.; Schmidt, H.-W. *Macromolecules* **2003**, *36*, 5150.
(18) Kristiansen, M.; Gress, A.; Smith, P.; Hanft, D.; Schmidt, H.-W. *Polymer* **2006**, *47*, 249.
(19) Thierry, A.; Straupe, C.; Lotz, B.; Wittmann, J. C. *Polym. Commun.* **1990**, *31*, 299.
(20) Kristiansen, M.; Tervoort, T.; Smith, P.; Goossens, H. *Macromolecules* **2005**, *38*, 10461.
(21) Sherpard, T. A.; Delsorbo, D. R.; Louth, R. M.; Walborn, J. L.; Norman, D. A.; Harvey, N. G.; Spontak, R. J. *J. Polym. Sci., Part B: Polym. Phys.* **1997**, *35*, 2617.
(22) Winter, H. H.; Chambon, F. *J. Rheol.* **1986**, *30*, 367.
(23) Winter, H. H. *Polym. Eng. Sci.* **1987**, *27*, 1698.
(24) Macosko, C. W. *Rheology*; VCH Publishers: New York, 1994.
(25) Nielsen, L. E. *Mechanical Properties of Polymers and Composites*; Marcel Dekker: New York, 1974.
(26) Stauffer, D.; Aharony, A. *Introduction to Percolation Theory*; Routledge: London, 1994.

MA060868V